Proceedings of the ASME 2010 3rd Joint US-European Fluids Engineering Summer Meeting and 8th International Conference on Nanochannels, Microchannels, and Minichannels
FEDSM-ICNMM2010
August 1-5, 2010, Montreal, Canada

FEDSM-ICNMM2010-30079

THE DYNAMICS OF CANTILEVERED FLEXIBLE PLATES IN AXIAL FLOW

Wensheng Zhao
School of Power and Mechanical Engineering
Wuhan University
Wuhan 430072, Hubei, PR China

Michael P. Païdoussis
Department of Mechanical Engineering
McGill University
Montréal, Québec, Canada H3A 2K6

Liaosha Tang
University of Toronto Institute for Aerospace Studies
Toronto, Ontario, Canada M3H 5T6

Meiqing Liu
School of Power and Mechanical Engineering, Wuhan University
Wuhan 430072, Hubei, PR China

Jin Jiang
School of Power and Mechanical Engineering, Wuhan University
Wuhan 430072, Hubei, PR China

ABSTRACT

A theoretical and experimental study has been conducted to investigate the dynamics of cantilevered flexible plates in axial flow. In this paper, a nonlinear equation of motion of plate based on the inextensibility assumption, coupled with an unsteady lumped vortex model for the aerodynamic part is used to analyze the dynamical behaviour of this fluid-structure system theoretically. Experiments have been conducted in a 3 ft × 2 ft wind tunnel, using polypropylene carbonate films, thin brass plates, polyester sheets, and type 304 stainless steel sheets, with maximum dimensions 22.4 cm × 16.8 cm. In the experiments, time traces, PSDs, phase-plane plots, Poincaré maps, PDFs, and autocorrelations are used to characterize the motions of the system. Periodic, period-doubling and chaotic oscillations have been observed. In the experiments, flutter arises via a subcritical bifurcation accompanied by hysteresis for low aspect ratio plates; the hysteresis disappears for large aspect ratio plates. The hysteresis phenomenon is considered to be due to three-dimensional bending of the plates. Furthermore, for flow velocities in the hysteresis loop, the stable plate subjected to a small external disturbance will flutter with the same amplitude limit cycle oscillation as self-excited oscillation at the same flow velocity. The experimental critical velocities for flutter onset are in good qualitative and quantitative agreement with the theoretically predicted values.

1. INTRODUCTION

All the previous extensive study on cantilevered flexible plates in axial flow showed that the system will lose stability through flutter at sufficiently high flow velocity. The fundamental and systematical study of cantilevered plates in axial flow may be found in a monograph by Dowell [1].The extensive literature on this topic has recently been reviewed by Païdoussis [2]. The first studies on cantilevered flexible plates in compressible and supersonic axial flow were undertaken by Dowell [3-6], and in essentially incompressible and subsonic by Taneda [7], Datta & Gottenberg [8], Kornecki et al. [9], and Shayo [10]. Recently, extensive investigations have been done on this classical topic by Huang [11], Guo & Païdoussis [12], Zhang [13], and Yamaguchi [14].

Theoretically, Kornecki et al. [9] used a linear beam model for the plate and Theodorsen's theory for the aerodynamics to study the system. Watanabe et al. [15] and Balint & Lucey [16] used a linear beam model of the plate and a two-dimensional Navier–Stokes solver to numerically simulate the system. Lemaitre et al. [17] used a linear beam model and slender wing theory to investigate the system. Yadykin et al. [18] used a nonlinear beam model based on the inextensibility condition and slender wing theory for the aerodynamics. Tang & Dowell [19-21] adopted a nonlinear structure model using the inextensibility condition and a two-dimensional vortex lattice model to study cantilevered plates in axial flow. Tang and Païdoussis [22, 23] used a nonlinear equation of the plate based on the inextensibility condition and unsteady lumped vortex model to investigate the nonlinear effects and limit cycle oscillations of fluttering plates in axial flow.

Experimentally, Taneda [7] conducted the earliest flutter experiments on a vertically hanging flag, Datta and Gottenberg [8] conducted similar flutter experiments on strips in airflow. Zhang et al. [13] conducted experiments on hanging filaments in a flowing soap film and observed the evolution of the wake vortices and its correlation to system stability. Lemaitre et al.

[17] conducted experiments on strips and found the critical flow velocity. Tang et al. [19] conducted experiments on cantilevered plates in axial flow and found good agreement with theory for the onset of flutter. Shelley et al. [24] conducted experiments in water flow and got results in qualitative agreement with theory for the critical flow speed.

In this paper, the main work is to complement the experimental research and validate the theoretical predictions in Tang and Païdoussis [22, 23]. The experiment was a two-dimensional cantilevered plastic plate immersed in axial flow. An optoNCDT laser sensor was used to measure the oscillation of the plate. Time traces, PSDs, phase-plane plots, Poincaré maps, PDFs, and autocorrelations were used to analyze the response. Furthermore, the hysteresis phenomenon was investigated. Good agreement of critical velocities for flutter onset between the theoretical and experimental values was achieved.

2. AEROELASTIC MODEL

A schematic of a cantilevered plate in axial flow is shown in Figure 1. The physical parameters of the two-dimensional plate are the length L, upstream clamped rigid segment of length L_0, thickness h, material density ρ_P and bending stiffness $D = Eh^3/[12(1-v^2)]$, where E is Young's modulus and v is the Poisson ratio; a is the coefficient of Kelvin-Voigt damping.

Based on the inextensibility assumption and following Semler et al. [25], the transverse displacement of the plate W is

$$\rho_P h\ddot{W} + D(1+a\frac{\partial}{\partial t})[W''''(1+W'^2)+4W'W''W'''+W''^3]$$
$$+\rho_P hW'\int_0^S(\dot{W}'^2+W'\ddot{W}')dS - \rho_P hW''\int_S^L\left[\int_0^S(\dot{W}'^2+W'\ddot{W}')dS\right]dS$$
$$= F_L - W'F_D + W''\int_S^L F_D dS\ , \tag{1}$$

where S is measured along the centreline of the plate. The longitudinal displacement of the plate V is

$$V = -\frac{1}{2}\int_0^S W'^2 dS\ . \tag{2}$$

In equations (1) and (2), F_L and F_D are, respectively, the transverse and longitudinal fluid loads acting on the plate, a is the Kelvin-Voigt-type material damping coefficient [26]. The overdot and the prime represent, respectively, temporal and spatial derivatives, i.e., $\partial(\ )/\partial t$ and $\partial(\ )/\partial S$.

Using plate length L as the length scale, $\sqrt{\rho_P hL^4/D}$ as the time scale, $\rho_F U^2$ as the fluid load scale to normalize the spatial and temporal variables, ρ_F being the fluid density,

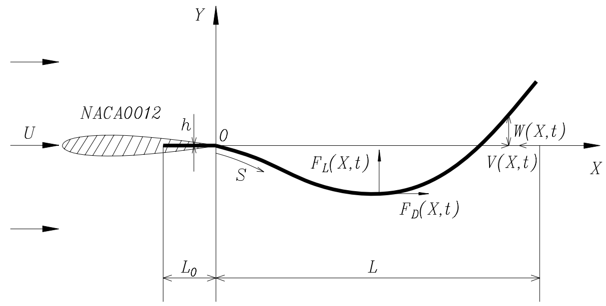

Figure 1. Schematic of the cantilevered plate in axial flow.

defining the mass ratio $\mu = \rho_F L/\rho_P h$, and the reduced velocity $U_R = UL\sqrt{\rho_P h/D}$, the non-dimensional plate equations of motion (1) and (2) are obtained as

$$\ddot{w} + (1+\alpha\frac{\partial}{\partial\tau})[w''''(1+w'^2)+4w'w''w'''+w''^3]$$
$$+w'\int_0^s(\dot{w}'^2+w'\ddot{w}')ds - w''\int_s^1\left[\int_0^s(\dot{w}'^2+w'\ddot{w}')ds\right]ds$$
$$= \mu U_R^2(f_L - w'f_D + w''\int_s^1 f_D ds)\ , \tag{3}$$

$$v = -\frac{1}{2}\int_0^s w'^2 ds\ , \tag{4}$$

where $w = W/L$, $v = V/L$, $s = S/L$, $\tau = t/\sqrt{\rho_P hL^4/D}$, $\alpha = a/\sqrt{\rho_P hL^4/D}$, $f_L = F_L/\rho_F U^2$, $f_D = F_D/\rho_F U^2$.

The flexible section of the plate is divided into N panels ("mesh segments"), each of length $\Delta s = 1/N$. Individual panels are put on the deformed contour of the plate centerline.

In equations (3) and (4), on the *i*th panel, the lift load on *i*th mesh segment $f_{Li} = \Delta p_i \cos\alpha_i$, and drag load on *i*th mesh segment $f_{Di} = \Delta p_i \sin\alpha_i + C_D$, where Δp_i is the pressure difference on *i*th mesh segment [27], α_i is angle between the *i*th segment and the abscissa. C_D is the non-dimensional drag coefficient used for the viscous drag acting on the plate.

The corresponding boundary conditions are

$$w(s=0,\tau)=0\ ,\quad w'(s=0,\tau)=0\ ,$$
$$w''(s=1,\tau)=0\ ,\quad w'''(s=1,\tau)=0\ . \tag{5}$$

The non-dimensional nonlinear partial equation of motion is discretized by the Galerkin method with the eigenfunctions of cantilevered beam as the fundamental functions. The resulting set of ordinary differential equations is then solved by Houbolt's finite difference method [28].

3. EXPERIMENTAL SET-UP

The schematic of the experimental set-up is shown in Figure 2. The cross-section of the wind tunnel is 3 ft × 2 ft. The maximum flow velocity is 39.8 m/s measured with a Pitot tube. The clamped support is a NACA0012 airfoil, the middle segment is made of aluminum and the ends of Delrin. The chord is 96.95 mm, the span is 619.8 mm. The cantilevered plates are made of four different materials: polypropylene carbonate films, thin brass plates, polyester sheets, and type 304 stainless steel sheets. The plates are sandwiched-in and clamped securely at the middle trailing edge of the airfoil. The length of the plates L varies from 60 mm to 224 mm. The width of the plates B varies from 60 mm to 200 mm. The length of clamped rigid segment is 50 mm. The flexural rigidity EI is measured by the method proposed by Païdoussis & Des Trois Maisons [29]. As the polypropylene carbonate films are transparent, they are sprayed with paint so that they can be used with the optoNCDT laser sensor. The characteristics of different materials are listed in Table 1.

The optoNCDT laser beam is pointed at a central spot at X=0.75L of the flexible section to measure the oscillation amplitude of plate. The output signals from the transducer are filtered and recorded by the data acquisition system, and the time traces, PSDs, phase-plane plots, Poincaré maps, PDFs, and autocorrelations are used to investigate the response of the system. A digital camera and a stroboscope are used to record the flutter mode shapes.

The flow velocity is gradually increased from naught to a high enough value. At the beginning, the cantilevered plate is stable; at a critical flow velocity, the plate begins to flutter. If we keep on increasing the flow velocity to a certain point, and then slowly decrease it, the behaviour is subcritical, i.e., stabilization occurs at a lower flow velocity than that for onset of flutter. During the whole process, the system shows periodic, period-doubling and chaotic oscillations.

The plate is gradually shortened to investigate the relationship of length L and critical velocity U_C.

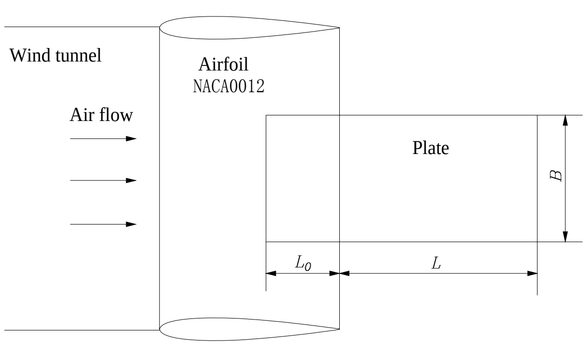

Figure 2. Schematic of the experimental set-up.

Table1. Characteristics of different materials

	h (mm)	ρ_P (kg/m^3)	EI (N·m^2)
Polypropylene films	0.12	1345	1.8×10^{-5}
Brass plates	0.1	8550	3.2×10^{-4}
Polyester sheets	0.127	1480	9.8×10^{-6}
Stainless steel sheets	0.127	7900	5.4×10^{-4}

4. RESULTS AND DISCUSSION

4.1 Typical Dynamics of a Cantilevered Plate

Typical results of cantilevered polypropylene films with L = 16 cm in axial flow at reduced velocity U_R = 8.05, U_R = 27.67 are presented separately in Figures 3 and 4: time traces, PSDs, phase-plane plots, Poincaré maps, PDFs, and autocorrelations. In Figure 3(a), the time trace shows that the limit cycle oscillation is almost periodic and harmonic. In Figure 3(b), the main oscillation frequency is f = 5.62 Hz. Figure 3(c) shows that the oscillation is periodic, as confirmed by the single point shown in the Poincaré map of Figure 3(d). In Figure 3(e), the PDF of the oscillation displays two symmetric prominent peaks at the extremes of the displacement, also characteristic of periodic motion. The autocorrelation in Figure 3(f) confirms this. Thus all the measures employed in Figure 3 indicate a periodic motion. In Figure 4(a, c), the time trace and the phase-plane plot show that the limit cycle oscillation is quite chaotic. In Figure 4(b), there is a main oscillation frequency at f = 42.82 Hz, but the low-frequency content is wide-banded and erratic. In Figure 4(d), the cluster of points in $(w, \dot{w})$- plot clearly shows that the oscillation is quite chaotic. In Figure 4(e), the prominent peaks disappear, and the PDF has become less concave. In Figure 4(f), the autocorrelation decays rapidly with time. The fuzzy multiple-loop phase-plane plot, the fuzzy points of Poincaré map, the convex shape of the PDF and the essentially rapidly decayed autocorrelation all indicate the chaotic motion of the system.

4.2 The Hysteresis in Flutter Onset and Cessation

The cantilevered plates may lose stability by flutter with increase of flow velocity via a subcritical Hopf bifurcation. When the flow velocity reaches a critical value, the cantilevered plates flutter suddenly with a large amplitude. While the cantilevered plates are already in oscillation, gradually reducing the velocity, the plates may return to stability at another critical velocity, which is lower than the former one; thus a hysteresis loop is formed. This type of hysteresis phenomenon has been mentioned in previous experimental research [13, 19, 22, 24, 30]. In Figure 5(a), the hysteresis with respect to flutter onset/cessation is observed for

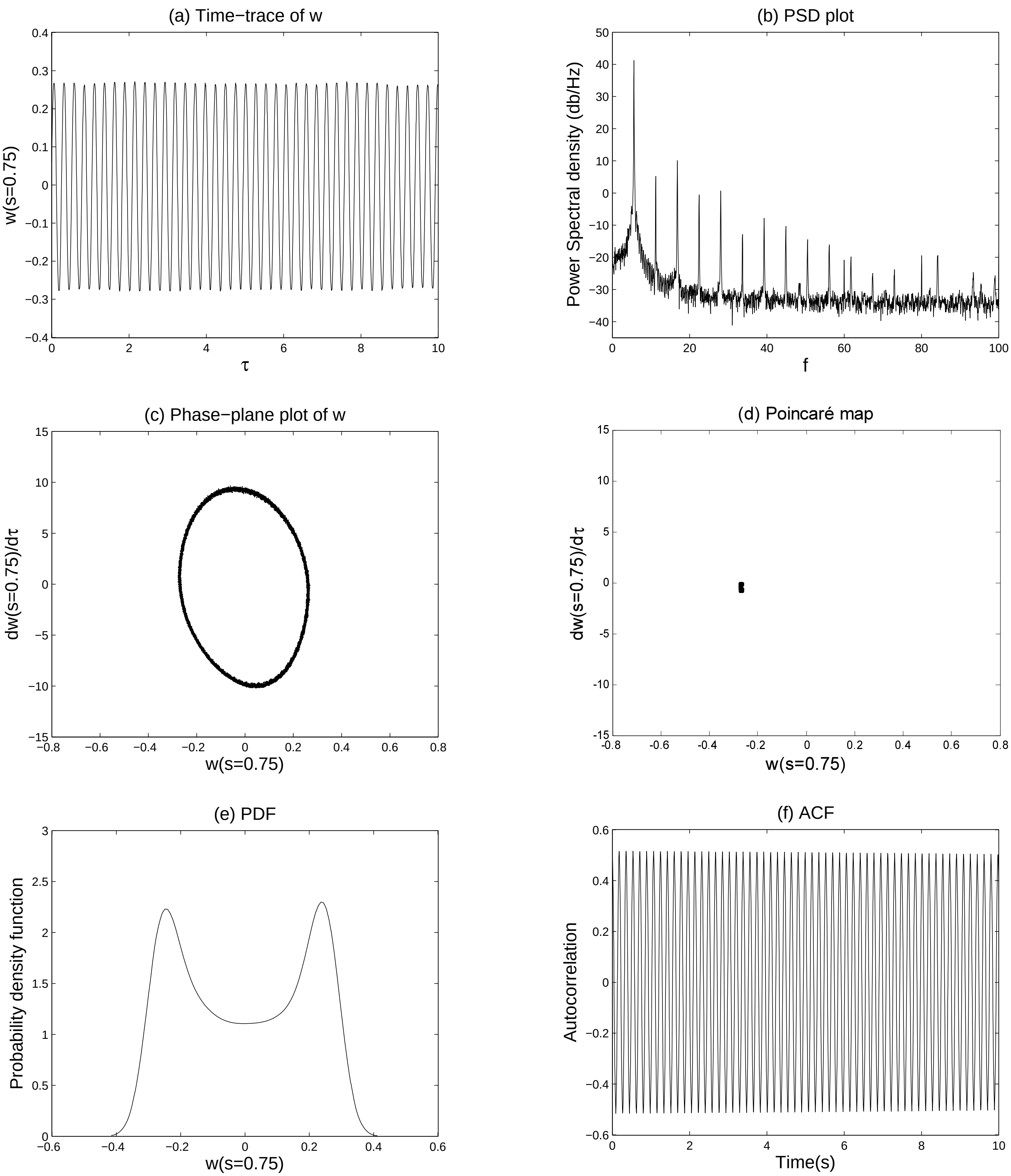

Figure 3. Experimental time trace of *w(s=0.75)*, power spectral density (PDF), phase-plane plot, Poincaré map, probability density function (PDF), and autocorrelation for cantilevered polypropylene carbonate film with L = 16 cm, B = 12 cm, μ = 1.215, U_R = 6.54.

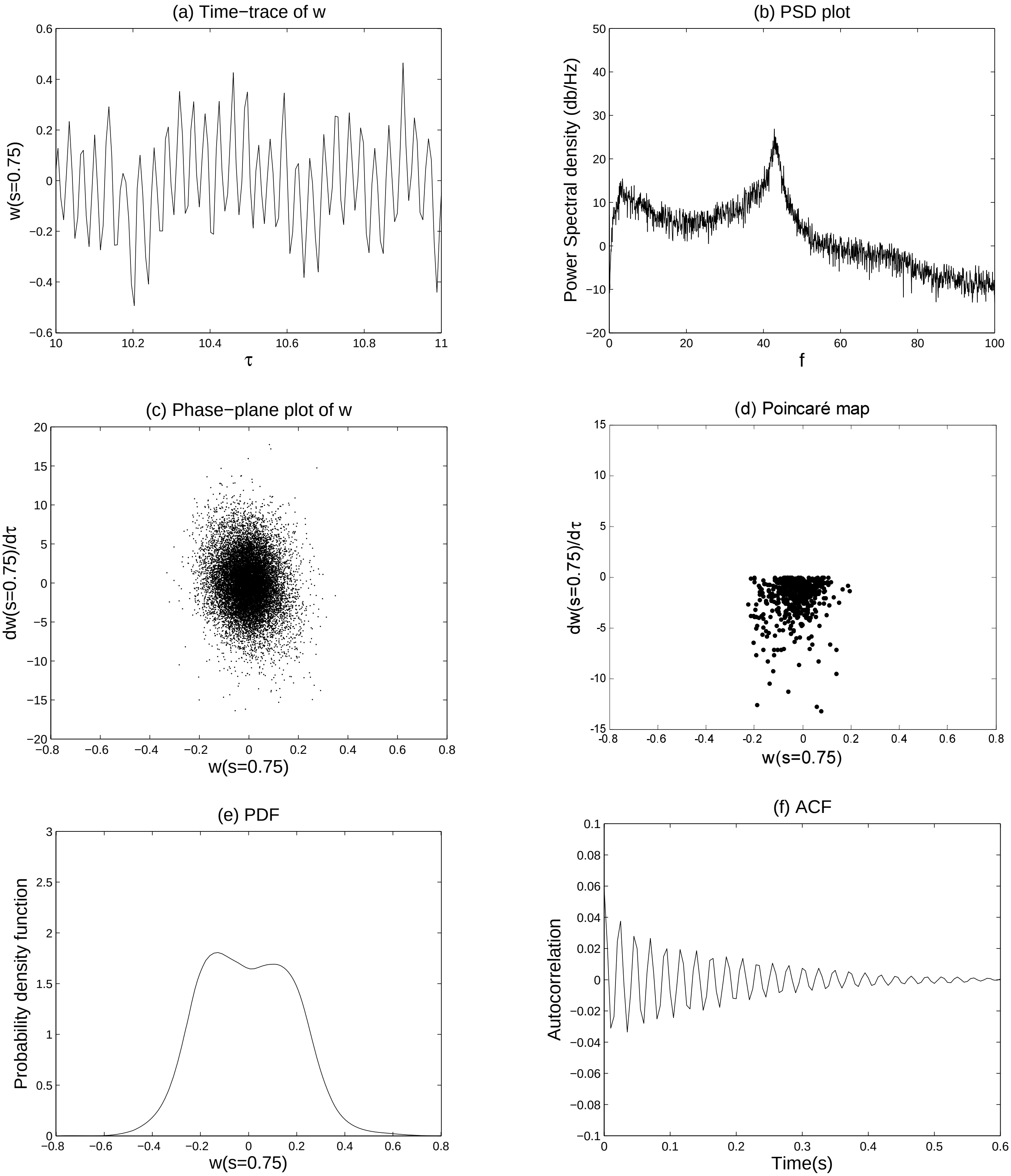

Figure 4. Experimental time trace of *w(s=0.75)*, power spectral density (PDF), phase-plane plot, Poincaré map, probability density function (PDF), and autocorrelation for cantilevered polypropylene carbonate film with *L* = 16 cm, *B* = 12 cm, *μ* = 1.215, U_R = 27.67.

a low aspect ratio plate, L/B=1. Furthermore, for flow velocities in the hysteresis loop, the stable plate subjected to a small external disturbance will flutter with the same amplitude limit cycle oscillation as self-excited oscillation at the same flow velocity, as illustrated by the dash-dot lines. The plate loses stability at a flow velocity U_{PRC} = 6.54, and returns to stability at a flow velocity U_{SRC} = 5.13. Thus, the bifurcation leading to flutter is subcritical in this case. In Figure 5(b), the hysteresis disappears for a large aspect ratio plate, L/B=1.33. The plate loses stability at critical velocity U_{RC} = 4.39, which is smaller than the critical velocity for the low aspect ratio plate. There are no existing theories capable of predicting the subcritical

(a)

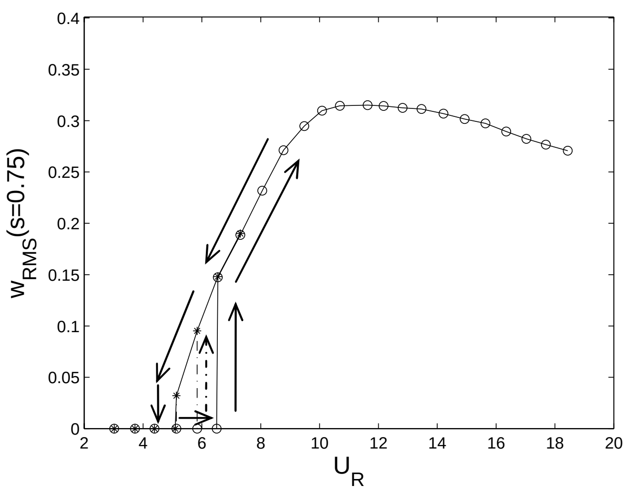

(b)

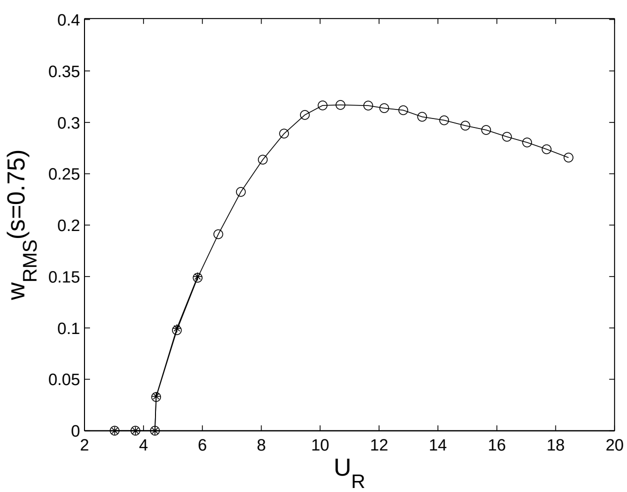

Figure 5. The bifurcation diagram of the system with *L* = 16 cm, *μ* = 1.215, (a) *B* = 16, (b) *B* = 12; —o—, velocity is increased, — · —, velocity is decreased.

flutter behaviour of cantilevered plates. Most of theories assume that the plates are two-dimensional, ignore the tension owing to the bending of plates, which will stiffen the plates. In the experiments, the three-dimensional bending of the low aspect ratio plates is clearly visible, while such 3-D bending for large aspect ratio plates is not obvious. It is therefore likely that the hysteresis phenomenon is due to the three-dimensional bending of the plates.

4.3 The Flutter Boundary

Figure 6 shows the flutter boundary of the system obtained both theoretically and experimentally. Other theoretically predicted flutter boundaries [11, 12, 14, 30] are also shown in the figure. In Figure 6(a), the mass ratio $\mu = [\rho_F / (\rho_P h) L]$, the ordinate is written as $U_{RC} / \mu = [(\rho_P h)^{3/2} / (\rho_F D^{1/2})] U_C$; as for a given situation, the parameters ρ_P , h , D , ρ_F are constants, we can investigate the effect of the plate length L on the critical velocity U_C. In Figure 6(b), $1/\mu$ is adopted to clearly show the critical velocities corresponding to small μ .

The theoretical and experimental flutter boundaries are in good qualitative and quantitative agreement with other predicted values. For short plates, i.e., $\mu < 1.2$, the dependence of the critical velocity U_C on the plate length L is strong; for long plates, i.e., $\mu > 1.5$, the dependence of the critical velocity on U_C on the plate length L is weak. When the plate length L is long enough, the critical velocity U_C converges to a nearly constant value; in the range $1.2 < \mu < 1.5$, the critical velocity U_C jumps up and down as L increases, which is caused by the transition of flutter mode in this range [30].

It is very noticeable that the experimental data is closest to Huang's theoretical predictions [11]. The main differences in Huang's model relative to present model are: (i) in Huang's theoretical method, an analytical model using Theodorsen's theory combined with a linear beam model is developed to predict the critical flow velocity, while in the present theoretical method a nonlinear equation of motion of the plate coupled with an unsteady lumped vortex model for the aerodynamics is used to predict the critical flow velocity; (ii) in Huang's theory, the effect of viscosity is embedded in the Kutta-Zhukovskii condition, while in the present theoretical study the effect of viscosity is incorporated in the drag F_D as a surface viscous force; (iii) in Huang's theory, the effect of the rigid upstream segment is not considered, while in the present theory the rigid upstream segment is included in the model. For a short rigid upstream segment l_0, the influence of l_0 on the critical flow velocity is significant [22]; (iv) in Huang's theory, the structural damping is neglected for the sake of producing a safe flutter boundary, while in the present theory the material damping is considered. When taking into account the material damping, the system becomes more stable.

(a)

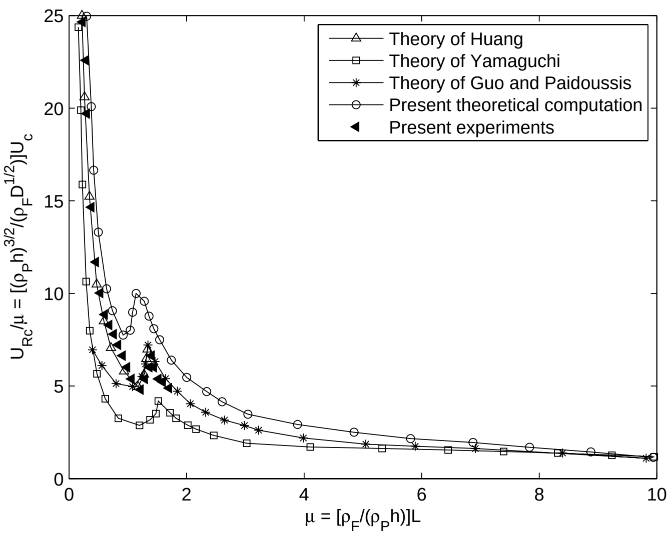

(b)

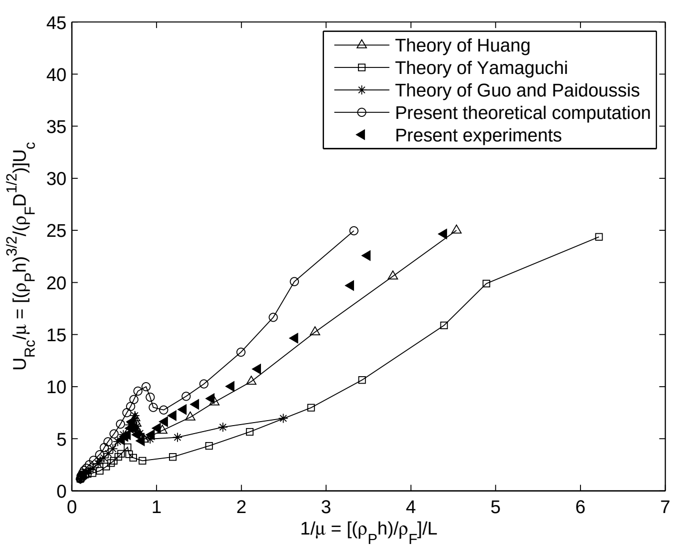

Figure 6. The flutter boundary of cantilevered flexible plates in axial flow, (a) μ vs. U_{RC}/μ, (b) $1/\mu$ vs. U_{RC}/μ.

5. CONCLUDING REMARKS

In this paper, the dynamics of cantilevered flexible plates in axial flow is investigated theoretically and experimentally.

In the experiment, as the flow velocity increases from naught, the cantilevered plates lose stability by a Hopf bifurcation. When the flow velocity exceeds the critical velocity, symmetric limit cycle oscillations occur, succeeded by a not so obvious period-doubling and then chaotic oscillations.

The hysteresis phenomenon is obvious for low aspect ratio plates; however, it is totally absent for large aspect ratio plates. Furthermore, in the hysteresis loop, the stable plate subjected to a small external disturbance will flutter with the same amplitude limit cycle oscillation as self-excited oscillation at the same flow velocity. The hysteresis phenomenon is considered to be due to the three-dimensional bending of the plates.

The dependence of the critical velocity on the plate length is strong for short plates, while the dependence is weak for long plates. The critical velocity converges to nearly a constant value when the plate length is sufficiently long. The critical velocity has a transition in a specific range of plate length. The current theory and experiments achieve good qualitative and quantitative agreement with other theories.

ACKNOWLEDGMENTS

The authors gratefully acknowledge the support by the Nature Science Foundation of China (Grant No. 50879062), the Natural Sciences and Engineering Research Council of Canada (NSERC), and the China Scholarship Council (CSC).

REFERENCES

[1] Dowell, E.H., 1975, Aeroelasticity of Plates and Shells, first ed., Noordhoff International Publishing, Leyden.

[2] Païdoussis, M.P., 2004, Fluid-Structure Interactions: Slender Structures and Axial Flow, Volume 2, Elsevier.

[3] Dowell, E.H., 1967, “Nonlinear oscillations of a fluttering plate, II,” AIAA Journal 5, pp. 1856-1862.

[4] Dowell, E.H., 1966, “Nonlinear oscillations of a fluttering plate,” AIAA Journal 4, pp. 1267-1275.

[5] Dowell, E.H., and Ventres, C.S., 1970, “Comparison of theory and experiment for nonlinear flutter of loaded plates,” AIAA Journal 8, pp. 2022-2030.

[6] Dowell, E.H., and Voss, H.M., 1965, “Theoretical and experimental panel flutter studies in the mach number range 1.0 to 5.0,” AIAA Journal 3, pp. 2292-2304.

[7] Taneda, S., 1968, “Waving motions of flags,” Journal of the Physical Society of Japan 24, pp. 392-401.

[8] Datta, S.K., and Gottenberg, W.G., 1975, “Instability of an elastic strip hanging in an airstream,” Journal of Applied Mechanics 42, pp. 195-198.

[9] Kornecki, A., Dowell, E.H., and Brien, J. O’, 1976, “On the aeroelastic instability of two-dimensional panels in uniform incompressible flow,” Journal of Sound and Vibration 47, pp. 163-178.

[10] Shayo L.K., 1980, “Stability of cantilever panels in uniform incompressible flow,” Journal of Sound and Vibration 68, pp. 341-350.

[11] Huang L.X., 1995, “Flutter of cantilevered plates in axial flow,” Journal of Fluids and Structures 9, pp. 127-147.

[12] Guo C.Q., and Païdoussis M.P., 2000, “Stability of rectangular plates with free side-edges in two-dimensional inviscid flow,” Journal of Applied Mechanics 67, pp. 171-176.

[13] Zhang J., Childress S., Libchaber A., and Shelley M., 2000, “Flexible filaments in a flowing soap film as a

model for one-dimensional flags in a two-dimensional wind," Nature 408, pp. 835-839.
[14] Yamaguchi N., Yokota K., and Tsujimoto Y., 2000, "Flutter limits and behaviours of a flexible thin sheet in high-speed flow – I: analytical method for prediction of the sheet behaviour," ASME Journal of Fluid Engineering 122, pp. 65-73.
[15] Watanabe, Y., Isogai, K., Suzuki, S., and Sugihara, M., 2002, "A theoretical study of paper flutter," Journal of Fluids and Structures 16 (2002), pp. 543-560.
[16] Balint, T.S., and Lucey, A.D., 2005, "Instability of a cantilevered flexible plate in viscous channel flow," Journal of Fluids and Structures 20, pp. 893-912.
[17] Lemaitre, C., Hémon, P., and de Langre, E., 2005, "Instability of a long ribbon hanging in axial air flow," Journal of Fluids and Structures 20, pp. 913-925.
[18] Yadykin, Y., Tenetov, V., and Levin, D., 2001, "The flow-induced vibration of a flexible strip hanging vertically in a parallel flow, part 1: temporal aeroelastic instability," Journal of Fluids and Structures 15, pp. 1167-1185.
[19] Tang D.M., Yamamoto H., and Dowell, E.H., 2003, "Flutter and limit cycle oscillations of two-dimensional panels in three-dimensional axial flow," Journal of Fluids and Structures 17, pp. 225-242.
[20] Tang, D.M., and Dowell, E.H., 2001a, "Effects of angle of attack on nonlinear flutter of a delta wing," AIAA Journal 39, pp. 15-21.
[21] Tang, D.M., and Dowell, E.H., 2001b, "Limit cycle oscillations of two-dimensional panels in low subsonic flow," International Journal of Nonlinear Mechanics 37, pp. 1199-1209.
[22] Tang, L., and Païdoussis, M.P., 2007, "On the instability and the post-critical behaviour of two-Dimensional cantilevered flexible plates in axial flow," Journal of Sound and Vibration 305, pp. 97-115.
[23] Tang, L., and Païdoussis, M.P., 2008, "Influence of the wake on the stability of cantilevered flexible plates in axial flow," Journal of Sound and Vibration 310, pp. 512-526.
[24] Shelley, M., Vandenberghe, N., and Zhang, J., 2005, "Heavy flags undergo spontaneous oscillations in flowing water," Physical Review Letters 094302, pp. 1-4.
[25] Semler, C., Li, G.X., and Païdoussis, M.P., 1992, "The non-linear equations of motion of pipes conveying fluid," Journal of Sound and Vibration 165, pp. 577-599.
[26] Snowdon, J.C., 1968, Vibration and Shock in Damped Mechanical Systems, 1st ed., Wiley, New York.
[27] Katz, J., and Plotkin, A., 2001, Low-Speed Aerodynamics, 2nd ed., Cambridge University Press, New York.
[28] Semler, C., Gentleman, W.C., and Païdoussis, M.P., 1996, "Numerical solutions of second order implicit non-linear ordinary differential equations," Journal of Sound and Vibration 195, pp. 553-574.
[29] Païdoussis, M.P., and Des Trois Maisons, P.E., 1971, "Free vibration of a heavy, damped, vertical cantilever," Journal of Applied Mechanics 38, pp. 524-526.
[30] Watanabe, Y., Suzuki, S., Sugihara, M., and Sueoka, Y., 2002, "An experimental study of paper flutter," Journal of Fluids and Structures 16, pp. 529-542.